

RSC Advances



This is an *Accepted Manuscript*, which has been through the Royal Society of Chemistry peer review process and has been accepted for publication.

Accepted Manuscripts are published online shortly after acceptance, before technical editing, formatting and proof reading. Using this free service, authors can make their results available to the community, in citable form, before we publish the edited article. This *Accepted Manuscript* will be replaced by the edited, formatted and paginated article as soon as this is available.

You can find more information about *Accepted Manuscripts* in the [Information for Authors](#).

Please note that technical editing may introduce minor changes to the text and/or graphics, which may alter content. The journal's standard [Terms & Conditions](#) and the [Ethical guidelines](#) still apply. In no event shall the Royal Society of Chemistry be held responsible for any errors or omissions in this *Accepted Manuscript* or any consequences arising from the use of any information it contains.

ARTICLE

A new chiral electrochemical sensor for the enantioselective recognition of Naproxen Enantiomers Using L-Cysteine Self-Assembled over Gold Nanoparticles at Gold Electrode

Abbas Afkhami*, Fatemeh Kafrashi, Mazaher Ahmadi and Tayyebeh Madrakian

Cite this: DOI: 10.1039/x0xx00000x

Received 00th January 2012,
Accepted 00th January 2012

DOI: 10.1039/x0xx00000x

www.rsc.org/

A chiral electrochemical sensor for the analysis of chiral compounds enantiomeric composition is reported. The method is based on the difference in the interaction of the naproxen (Nap) enantiomers with the chiral modified electrode surface. A chiral surface was synthesized on a gold electrode modified with gold nanoparticles and L-cysteine self-assembled monolayers (SAMs). Scanning electron microscopy (SEM), cyclic voltammetry (CV) and electrochemical impedance spectroscopy (EIS) were used to study the enantioselective interaction between the chiral surface and Nap enantiomers. The results showed that the modified electrode can be better stereoselective for S-Nap than for R-Nap. The examination of the characteristics of the chiral interface, including the response time, the effect of enantiomers concentration, and the stability, were investigated. Then the chiral selective interface was used to determine the Nap enantiomers mixtures by measuring the change in the peak current in different compositions from them. The results suggested that the proposed chiral biosensor with high sensitivity and selectivity can be used to the recognition of Nap enantiomers.

Introduction

Recognition of the chiral drugs is an important and attractive subject in the field of life science since individual isomers of a drug often differ in their bioactivity pharmacological activity and undergo different pharmacokinetic and metabolic fates in the biological systems.^{1,2} The enantiomers of a chiral molecule may exhibit different biological activities. One of the enantiomers is effective, while the other may be ineffective or even cause serious side-effects.³ Chemical analysis of chiral compounds, due to different physiological and therapeutic properties of their enantiomers, is the concern of science and technology researchers.^{4,5}

Naproxen (Nap), i.e., 2-(6-methoxy-naphthyl) propanoic acid, is a member of the 2-arylpropionic acid (profen) family of non-steroidal anti-inflammatory drugs (NSAIDs). NSAIDs including Nap are commonly employed to reduce ongoing inflammation, pain and fever, since they are able to block⁶ the cyclo-oxygenase (Cox) enzymes (Cox-1 and Cox-2), that both produce prostaglandins; these classes of compounds have several important functions, as the promotion of amputation, pain and fever.⁷ Nap is extensively used in the treatment of many diseases like rheumatoid arthritis, degenerative joint disease, ankylosing spondylitis, acute gout and primary

dismenorrhea.⁸ The pharmaceutical activity of S-naproxen (S-Nap) is 28 times stronger than that of R-naproxen (R-Nap) while R-Nap gives rise to some undesirable side-effects.⁹ Thence, chiral analysis of naproxen enantiomers in the presence of each other is important.

Various methods have been used to chiral analyses, including spectrofluorometry¹⁰ and resonance Rayleigh scattering (RRS)¹¹ after solid phase extraction, high performance liquid chromatography (HPLC)¹²⁻¹⁴, gas chromatography¹⁵, capillary electrophoresis (CE)¹⁶, chiral ligand exchange chromatography (CLEC)¹⁷, fluorescence detection^{18,19} mass spectrometry²⁰, NMR spectrometry²¹, near infrared spectrometry²², room temperature phosphorescence²³, molecular imprinting polymers chiral stationary phase²⁴ and electrochemical methods.²⁵

Recently, electrochemical techniques were used to chiral analysis of different enantiomers. Electrochemical methods have a lot of advantages such as low cost, high sensitivity and simplicity. Several electrochemical methods have been reported for the analysis of enantiomer compositions. Huang et al. fabricated a chiral sensor with a nanostructured composite for enantioselective recognition of lysine enantiomers.²⁶ Chen et al. reported a gold electrode modified by Cu(II) and L-cysteine for chiral recognition of tryptophan enantiomers.²⁷ Nie et al. constructed a chiral electrochemical sensor via cysteic acid modified glassy carbon electrode to discriminate tyrosine enantiomers.²⁸ Guo et al. designed chiral sensor for

enantioselective recognition of Nap enantiomers using BSA biofunctionalized reduced graphene oxide nanosheets.²⁹ Chen et al. fabricated a chiral electrochemical sensor through chemical linking L-methotrexate onto the gold electrode surface for the enantioselective recognition of penicillamine enantiomers.³⁰ Zhang et al. constructed a chiral electrochemical sensor by means of adsorbing human serum albumin onto a methylene blue-multi-wall carbon nanotubes nanohybrid modified glassy carbon electrode for the discrimination of tryptophan enantiomers.³¹

Persent sensor with high sensitivity, simplicity, low cost, low-power requirements, and high compatibility has been a preferable approach for chiral recognition of Nap enantiomers.

One of the principal goals to chiral recognition is to construct an effectual chiral selective system, which should have recognition site for certain chiral enantiomers.

In this work, a chiral surface was synthesized by a gold electrode modified with cysteine self-assembled monolayers (SAMs) over gold nanoparticles. The self-assembly procedure is a modification method of the surface of the electrodes which have been used for improvement of sensors and biosensors, that it leads to spontaneous chemisorption of the thiol groups on the gold surfaces.

Gold nanoparticles have potential applications in the construction of electrochemical sensors and biosensors³² because of their small dimensional size, good stability, biocompatibility, good conductivity and excellent catalytic activity.³³ On the other hand, gold nanoparticle modifications can greatly increase the immobilized amount of S-functionalized compounds and enhance the Au-S bond and stability of SAMs.³⁴ Also, electrochemical deposition of gold nanoparticles (AuNPs) is a fast and convenient method of preparation.^{35, 36}

Gold nanoparticles synthesis was performed by electrodeposition method at a constant potential, then L-cysteine was self-assembled on modified electrode. Cysteine, a small thiol-containing amino acid, contains carboxyl, amino and thiol functionalities³⁷ with a chiral centre. Since the interaction between two enantiomers of Nap and chiral interface is different, Nap enantiomers can be recognized. The scanning electron microscope (SEM), cyclic voltammetry (CV) and electrochemical impedance spectroscopy (EIS) were used to analyze the characteristics of the interface. The results showed that the modified electrode could be used to discriminate Nap enantiomers, and the chiral surface has good response for quantitative analysis of enantiomer compositions in the pharmaceutical samples. Also the modified electrode can be used to determine the concentration ratio of Nap enantiomers in the racemic mixtures.

Experimental

Reagents and materials

L-Cysteine (L-Cys), R- and S-Nap, L- and D-Tryptophan (Trp), L- and D- Alanine (Ala), L- and D- Histidin (His), L- and D- Proline (Pro), $\text{KAu}(\text{CN})_4$, $\text{K}_3[\text{Fe}(\text{CN})_6]$, $\text{K}_4[\text{Fe}(\text{CN})_6]$ and other chemicals were supplied by Aldrich Chem. Co.

(Milwaukee, WI, USA). Phosphate buffer was prepared by KH_2PO_4 and K_2HPO_4 which contained 0.1 M KCl (PBS, pH=6). All other reagents were commercially available and of analytical grade. Double distilled water was used throughout the experiments.

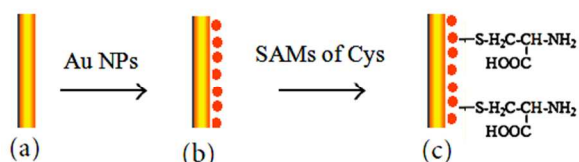
Apparatus

Cyclic voltammetry (CV) and electrochemical impedance spectroscopy (EIS) measurements were performed with a potentiostat/galvanostat (Autolab PGSTAT302 N) and it was controlled by a computer using Nova version 1.7 software. A conventional three electrodes system was employed with a bare or modified gold electrodes (Au, $\Phi = 4$ mm) as the working electrodes, a platinum wire auxiliary electrode as the counter electrode and an Ag/AgCl electrode as the reference electrode. Cyclic voltammetry and electrochemical impedance spectroscopy were measured in 2.5 mM $[\text{Fe}(\text{CN})_6]^{4-/3-}$ solution. Mira FEG-SEM, TESCAN instrument was used to obtain the scanning electron micrographs (SEM) of the different surfaces. All measurements were performed at room temperature.

Preparation of the working electrode

The gold electrode was polished with 1.0, 0.3, and 0.05 μm alumina slurries, and sonicated in double distilled water, ethanol, and double distilled water each for 5 min. Then the electrode was transferred to the electrochemical cell for cleaning by several potential cycling between -0.25 and $+1.6$ V vs. Ag/AgCl at 1 V s^{-1} in 0.5 M H_2SO_4 for 10 cycles and running 10 cycles in a fresh 0.5 M H_2SO_4 at 0.1 V s^{-1} with the same potential range, subsequently rinsed with double distilled water. At last, the pre-treated electrode was immersed in a solution containing 6 mmol L^{-1} $\text{KAu}(\text{CN})_4$ and 0.1 mol L^{-1} KNO_3 . The potential applied between the working electrode and Ag/AgCl electrode as the reference electrode was held constant at -400 mV (Bulk electrolysis, BE) for 400 s.²⁶ This electrode is denoted as Au/Au NPs.

A self-assembly monolayer of cysteine was formed on bare Au electrode and gold nanoparticles modified electrode (Au/Au NPs) by soaking the electrodes in 5 mmol L^{-1} L-cysteine/ 0.1 mol L^{-1} PBS/pH 2.58 for 15 min at room temperature.²³ These electrodes are denoted as Au-Cys and Au/Au NPs-Cys, respectively. The modified electrodes were washed with doubly distilled water to remove the physically adsorbed species and dried carefully without touching the surface. Scheme 1 shows the stepwise preparing of the modified electrodes.



Scheme 1 Schematic model of the chiral surface fabrication process (a) bare Au, (b) Au/AuNPs, (c) Au/AuNPs/Cys

Results and discussion

SEM measurements

The scanning electron microscope (SEM) was used for the modified electrode surface morphology characteristics. Fig. 1 display SEM images of stepwise preparing of the modified electrodes. The SEM images of Au/AuNPs and Au/AuNPs/Cys electrodes are shown in Figs. 1A and 1B, respectively. As seen in Fig. 1A, Au nanoparticles are randomly formed electrochemically and increased surface area. The shape and sizes of nanoparticles are not homogenous. The diameter of the synthesized nanoparticles were around 18–51 nm. Also in Fig. 1B cysteine molecules are assembled on the electrode surface.

These results confirm the existence of AuNPs on the modified electrode surface and also self-assembly of cysteine with sulfide groups.

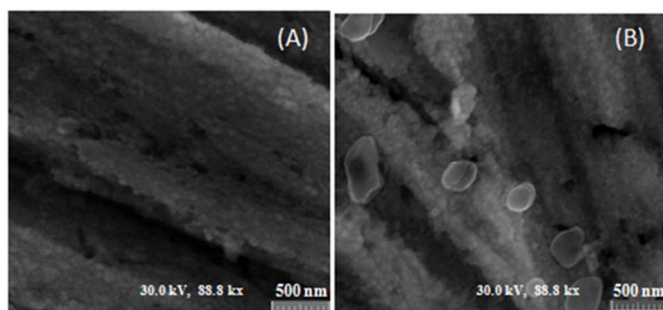


Fig. 1. SEM images of modified electrodes: A) Au/Au NPs; B) Au/Au NPs/Cys

Electrochemical characterization of the modified electrodes

The cyclic voltammetry of ferricyanide is a valuable and convenient tool to monitor the barrier of the modified electrode. It was used to study the interface properties of the modified electrodes. The cyclic voltammograms (CVs) of different modified electrodes in 2.5 mM $[\text{Fe}(\text{CN})_6]^{4-/3-}$ solution at a scan rate of 100 mV s^{-1} are shown in Fig. 2A. As can be seen, the reversible one-electron redox behavior of ferricyanide ions was observed on the bare gold electrode at the scan rate of 100 mV s^{-1} . After deposition of Au nanoparticles at the surface of gold electrode (Au/AuNPs electrode) the peak current increased. The increase in peak currents is due to the increase in the electrode surface of the electrode by electrodeposition of the Au NPs. After a self-assembly of the monolayer of cysteine at the gold nanoparticles modified electrode (curve c) the redox peak

current decreased a little while ΔE_p increased ($\Delta E_p = 110 \text{ mV}$). This indicates that the self-assembled cysteine monolayer partly blocked the electron-transfer of $[\text{Fe}(\text{CN})_6]^{4-/3-}$ at the gold electrode surface so the redox current decreased and the oxidation and reduction potentials increased.

The results of IES for the bare Au electrode, Au/Au NPs electrode and Au/Au NPs-Cys electrode in the presence of 2.5 mM $[\text{Fe}(\text{CN})_6]^{4-/3-}$ in 0.1 M KCl are shown in (Fig. 2B). It can be seen that bare Au electrode displays a semicircle part at high frequency region. Charge transfer resistance (R_{ct}) was estimated to be 930Ω . After being modified with Au nanoparticles, the semicircle diameter of EIS decreased and R_{ct} decreased to 566Ω , indicating that Au nanoparticles are deposited at Au electrode surface. After self-assembly of the monolayer of cysteine, R_{ct} was founded to be 1131Ω .

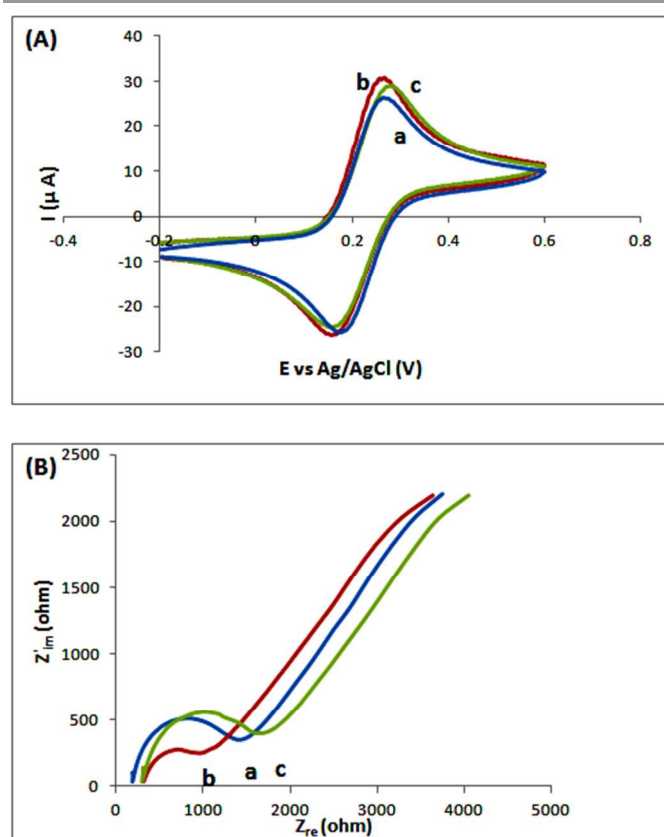


Fig. 2. (A) CV (a) Au, (b) Au-Au NPs, (c) Au-Au NPs-cys electrode. Scan potential: -0.20 to 0.6 V vs. Ag/AgCl. Scan rate: 100 mV s^{-1} . (B) EIS at different electrodes, in 0.1 M KCl containing 2.5 mM $[\text{Fe}(\text{CN})_6]^{4-/3-}$ solutions at $+0.25 \text{ V}$ from 0.1 Hz to 10.0 kHz.

The CVs of the Au-Au NPs-cys electrode in $[\text{Fe}(\text{CN})_6]^{4-/3-}$ solution at different scan rates were studied. The peak potential and current depended on the scan rate. A linear relationship between the oxidation peak current (I_p) with the square root of

the scan rate ($v^{1/2}$) in the range 60–400 mV s^{-1} confirms a diffusion control for electrochemical process.

Furthermore, the stability of the modified electrodes was studied. After 50 cycle CV measurements in $[\text{Fe}(\text{CN})_6]^{4-/3-}$ at 100 mV s^{-1} , the relative standard deviation (RSD) of peak currents was 0.65% ($n = 5$), indicating a good stability of this interface.

Also the reversibility of the sensor was investigated. After immersion of the chiral sensor in a 100 mg L^{-1} R- or S-Nap solution for 20 min and then immersing it in $[\text{Fe}(\text{CN})_6]^{4-/3-}$ solution, the peak current reached 99.2% of the blank peak current value (before immersing in enantiomer solution) then after 5 cycles CV measurements, the peak current reached at 99.7% of the blank value after 10 cycles CV. Thus sensor indicated a good reversibility.

Enantioselective recognition of Nap enantiomers

THE CV RESPONSE

Under the optimum experimental conditions, the enantioselective recognition for Nap enantiomers was carried out by the fabricated chiral biosensor. Fig. 3 shows the cyclic voltammograms for the Au/Au NPs-Cys modified electrode in a solution of 2.5 mM $[\text{Fe}(\text{CN})_6]^{4-/3-}$ at the scan rate of 100 mV s^{-1} before (curve a) and after immersion in 100 mg L^{-1} R-Nap (curve b) and S-Nap (curve c) solutions for 20 min. As shown in Fig. 3, the redox peak currents decreased and larger decrease was obtained from curve c than curve b (the current changed from 29.6 μA to 27.7 μA and 19.3 μA for R-Nap and S-Nap, respectively) that indicates presences of an interaction between L-Cys and R- or S-Nap, but the interaction of R-Nap was weaker than that for S-Nap. This is because the higher amount of R-Nap than S-Nap became adsorbed at the surface of chiral electrode and making a larger blocking layer for the electron transfer at the surface of the electrode. The change in current response for S-Nap ($\Delta I_S = I - I_S$, where I and I_S are the peak current before and after submerging the electrode in S-Nap solution, respectively), was found to be 10.3 μA , while the change in current response for R-Nap solution, ΔI_R ($\Delta I_R = I - I_R$, where I_R denotes the peak current after submerging the electrode in R-Nap solution) was found to be 1.9 μA . The difference between the current response change for R-Nap (ΔI_R) and S-Nap (ΔI_S), ΔI_{RS} ($\Delta I_{RS} = I_R - I_S$), was calculated as 8.4 μA . Such a large difference made the developed chiral biosensor effective in enantioselective recognition for Nap enantiomers. The results indicated that S-Nap bounds more strongly than R-Nap.

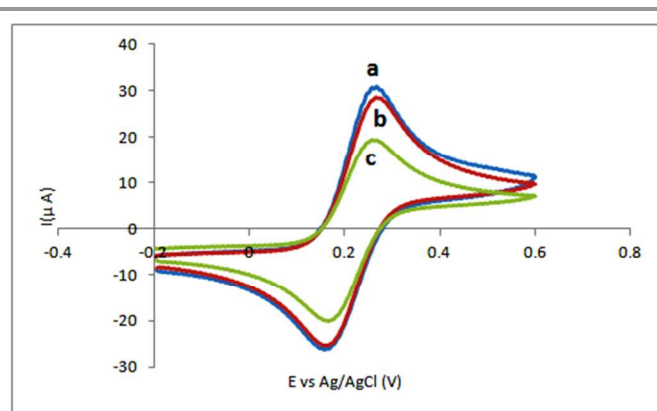


Figure 3. CVs for the modified electrode in 0.1 M KCl containing 2.5 mM $[\text{Fe}(\text{CN})_6]^{4-/3-}$ solutions (a) before and (b) after incubation R-Nap and (c) S-Nap, 100 mg L^{-1} , in Scan potential: -0.20 to 0.6 V vs. Ag/AgCl. Scan rate: 100 mV s^{-1} , pH = 6, Time of incubation = 20 min.

EIS MEASUREMENTS

EIS is usually used to probe the interfacial properties of the modified electrodes.³⁸ In EIS, the total impedance is determined by several parameters: (1) electrolyte resistance, R_s ; (2) the lipid bilayer capacitance, C_{dl} ; (3) charge transfer resistance, R_{ct} , and (4) Warburg element, Z_w . A modified Randles equivalent circuit was used to fit the measured results (inset of Fig. 4). R_s and Z_w represent bulk properties of the electrolyte solution and diffusion of the applied redox probe, respectively, which are not affected by chemical transformations occurring at the electrode interface. C_{dl} depends on the dielectric permittivity introduced into the double-charged layer molecules, and for the less polar molecules the capacitance should be smaller. R_{ct} depends on the insulating features at the electrode/electrolyte interface. The semicircle diameter in the impedance spectrum equals the interfacial electron transfer resistance (R_{ct}).²⁷ Fig. 4 illustrates the electron-transfer resistance of the modified electrodes before and after immersion in 100 mg L^{-1} R- or S-Nap solutions for 20 min. After interaction of the modified electrode ($R_{ct} = 1.13$ $\text{k}\Omega$, curve a) with R-Nap or S-Nap, the R_{ct} increased. Interaction of the electrode and enantiomers of Nap results in diminishing of the electron transfer of the ferrocyanide/ferricyanide. Also because of stronger interaction of S-Nap ($R_{ct} = 1.971$ $\text{k}\Omega$, curve c) than R-Nap ($R_{ct} = 1.481$ $\text{k}\Omega$, curve b) the electron-transfer resistance is larger. These results are consistent with those obtained from CV.

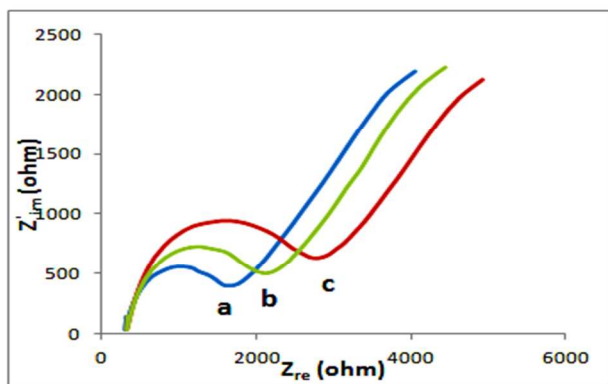


Figure 4. EIS for the modified electrode in 2.5 mM $[\text{Fe}(\text{CN})_6]^{4-/3-}$ solutions containing 0.1 M KCl (a) before and (b) after incubation in 100 mg. L⁻¹ R-Nap and (c) S-Nap. Scan potential: -0.20 to 0.6 V vs. Ag/AgCl. Scan rate: 100 mV·s⁻¹, pH = 6, Time of incubation = 20 min.

Optimization of the experimental condition

INFLUENCE OF THE pH

The pH of the solution plays an important role in enantiospecificity of Nap enantiomers. The effect of pH in the electrochemical response of the chiral biosensor was studied over the pH range 3 to 9 (Fig. 5A). It can be seen that the maximum difference of peak current between two enantiomers appeared at pH 6.0. Therefore, all experiments were performed in pH 6.0.

INFLUENCE OF THE INTERACTION TIME

Furthermore, the influence of the interaction time was studied from 5 to 30 min. As Fig. 5B shows, by increasing the interaction time of the S-Nap or R-Nap enantiomers the peak current change increased for both the enantiomers, and then tended to level off with the increase of reaction time. So, interaction time of 20 min was selected as the optimum time.

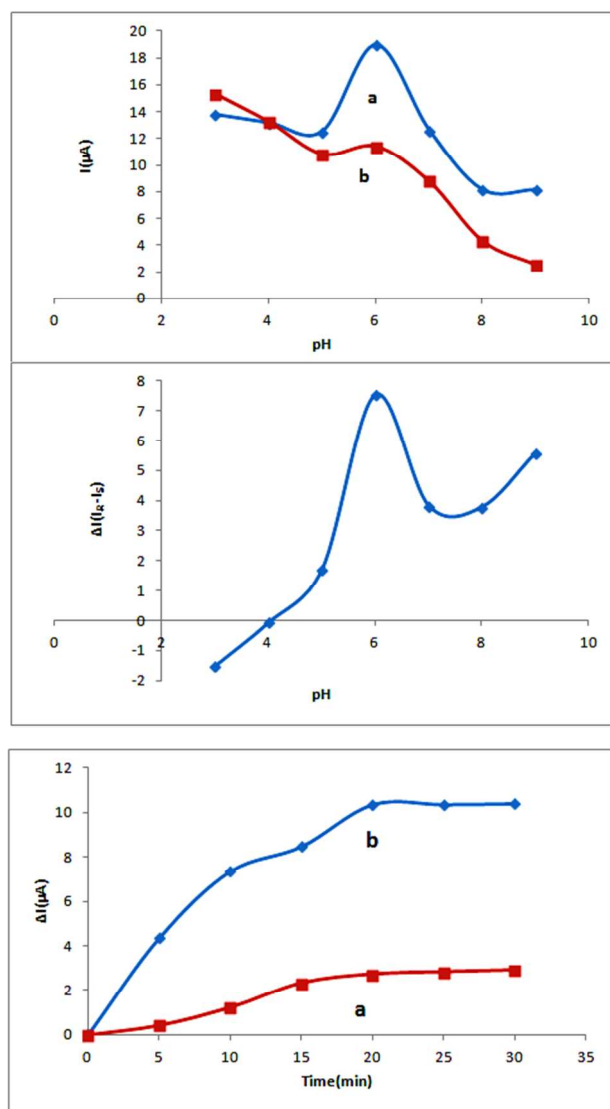


Figure 5. (A) The effect of pH on the peak current change of the chiral biosensor. From a to g: pH 3.0, 4.0, 5.0, 6.0, 7.0, 8.0, 9.0. (B) dependence of ΔI_p on pH and (C) dependence of the peak current change to time incubated (a) R-Nap and (b) S-Nap. in Scan potential: -0.20 to 0.6 V vs. Ag/AgCl. Scan rate: 100 mV·s⁻¹.

Enantioselectivity coefficient of the chiral biosensor

The selectivity of the chiral biosensor was quantitatively evaluated using the enantioselectivity coefficient (α), which is defined using the following equation:¹²

$$\alpha = \Delta I_S / \Delta I_R$$

where α is the enantioselectivity coefficient, a quantitative measure of a sensor's ability to discriminate the S-isomer from the interfering R-isomer, ΔI_S and ΔI_R are the differences in the anodic peak current after immersion of the modified electrodes, corresponding to the S- and R-naproxen, respectively.

The enantioselectivity coefficient for the chiral sensor was calculated as 5.4.

Four different chiral amino acids (tryptophan, alanine, histidine and proline) were also examined under the same conditions to investigate the selectivity of the chiral sensor. Table 1 shows the average differences in the anodic peak current and the enantioselectivity coefficient for the chiral sensor corresponding to the different amino acid enantiomers. The results showed that the sensor have good selectivity and specificity for Nap enantiomers.

To the best of our knowledge, only one report has been published on the introduction of an enantioselective electrochemical sensor for Nap.²⁹ The proposed sensor was compared with the reported one. As Table 2 shows, the obtained enantioselectivity coefficient for the proposed sensor is more than 2.5 times greater than that for the reported one.

Table 1 Enantioselectivity coefficient (α) of the chiral sensor corresponding to the amino acids enantiomers

Chiral analyte	ΔI_s (mA)	ΔI_R (mA)	α
Nap	10.3	1.9	5.4
Trp	9.2	3.4	2.7
Pro	10.5	7.8	1.3
His	6.6	5.6	1.2
Ala	6.4	6.1	—

Table 2 Comparison of the enantioselective electrochemical sensors for naproxen enantiomers

Types of electrode	Detection method	Linear range ($\mu\text{mol L}^{-1}$)	LOD ($\mu\text{mol L}^{-1}$)	α	Ref.
TBO@rG O/GCE	CV	500 to 5000	0.33	2.29	[29]
L-CYS/Au NPs/Au E	CV	2 to 20	0.67	5.4	This work

INFLUENCE OF NAPROXEN CONCENTRATION

Cyclic voltammetry measurements were performed over the different concentrations of S-Nap and R-Nap. As shown in Fig. 6, the relationship between the anodic peak current change and concentration of Nap enantiomers was a linear relationship. By increasing the concentration of S-Nap in the range 2.0×10^{-6} mol L⁻¹ to 2.0×10^{-5} mol L⁻¹, peak current increased with the linear equation, $I_p (\Delta I_s) (\mu\text{A}) = 0.5627 C (\mu\text{M}) + 0.5463$ ($R = 0.9701$). The $[\text{Fe}(\text{CN})_6]^{4-3-}$ solution peak current changed after immersion of the electrode in R-Nap solution for 20 min. Also peak current change increased linearly by increasing S-Nap concentration and the linear equation was $I_p (\Delta I_R) (\mu\text{A}) = 0.0702 C (\mu\text{M}) + 0.0496$ ($R = 0.9836$). The detection limit was obtained as 6.7×10^{-7} mol L⁻¹ ($S/N = 3$). As seen, an increase in the concentration of both the enantiomers caused an increase in current change at the modified electrode, but S-Nap caused a larger current change than R-Nap. Therefore, chiral biosensor could enantioselectively recognize Nap enantiomers.

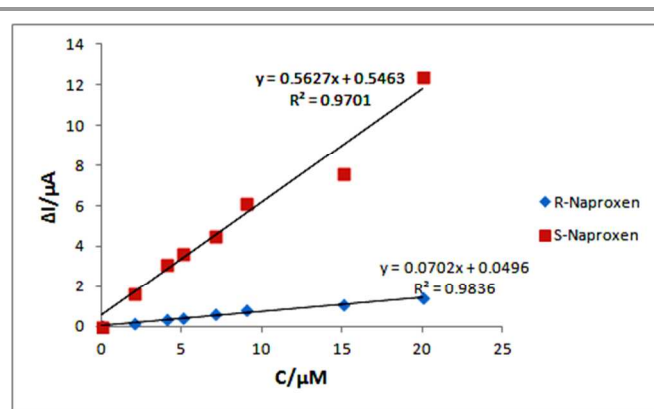


Figure 6: The relative change of oxidation current peak for different concentrations of naproxen enantiomers adsorbed on modified electrode (a) S-naproxen and (b) R-naproxen.

Application of the enantioselective electrode

Herein, the application of chiral biosensor was studied. The different volume ratios of S- and R-Nap mixing solutions were prepared. The peak current change gradually increased by increasing the ratio of S-Nap enantiomer to R-Nap for both high and low concentrations (Fig. 7). As seen, the modified electrode surface displayed higher chiral sensitivity to determine S-Nap rather than its counter isomer in the mixture solution. Also the calibration curves showed good linearity, the chiral biosensor can be used to determine one enantiomer of naproxen in the presence of the other isomer.

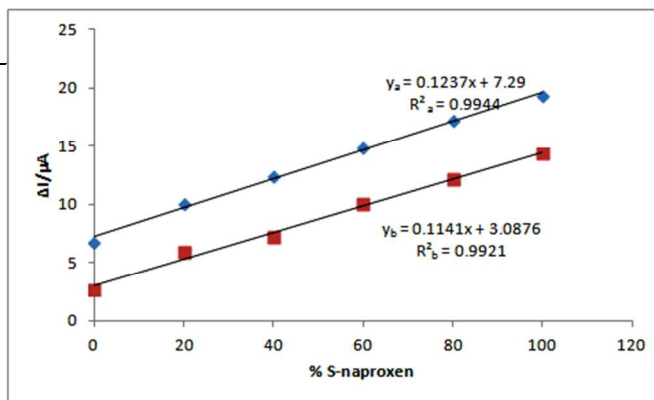


Figure 7: The relative change of the modified electrode oxidation current peak with enantiomeric composition of R- and S-naproxen at concentrations (a) 100 mg .L⁻¹ (b) 50 mg .L⁻¹

Conclusion

The present study demonstrates an excellent sensor based on L-Cys-SAMs on Au NPs/Au electrode for recognizing of one of the enantiomers of Nap in the presence of the other optical isomer. The modified electrode could be used successfully to enantioselective sensing of S-Nap in the presence of R-Nap. The results showed that larger decrease in the electrochemical signal was obtained from S-Nap than from R-Nap. The chiral

recognition was based on the different interaction of the Nap enantiomers with chiral modified electrode surface. The electrochemical response of a series of different concentrations of R- and S-Nap was measured, and a linear relation was observed between the peak current and concentration of Nap enantiomers. Of course, the slope of the calibration curve for S-Nap was larger than that for R-nap. On the other hand, the signal of nap enantiomers mixtures was investigated in different percent from them.

Acknowledgements

The authors acknowledge the Bu-Ali Sina University Research Council and Centre of Excellence in Development of Environmentally Friendly Methods for Chemical Synthesis (CEDEFMCS) for providing support to this work.

Notes

Faculty of Chemistry, Bu Ali Sina University, Hamedan, Iran.
E-mail: afkhami@basu.ac.ir Tel. /fax: +98 811 8272404.

References

- M. Zhang and B. C. Ye, *Anal. Chem.*, 2011, **83**, 1504-1509.
- M. Trojanowicz and M. Kaniewska, *Electroanalysis*, 2009, **21**, 229-238.
- T.Q. Yan, C. Orihuela, *J. Chromatogr. A*, 2007, **1156**, 220-227.
- G. Absalan and Y. Alipour, *J. Pharm. Biomed. Anal.*, 2013, **83**, 96-100.
- A. Afkhami, M. Abbasi-Tarighat and M. Bahram, *Talanta*, 2008, **75**, 91-98.
- Y. Sun, Z. Zhang, Z. Xi and Z. Shi, *Talanta*, 2009, **79**, 676-680.
- T. Madrakian, M. Ahmadi, A. Afkhami and M. Soleimani, *J. Analyst.*, 2013, **138**, 4542-4549.
- P. A. Todd and S. P. Clissold, *Drugs*, 1990, **40**, 91-137.
- F. Dimiza, A. N. Papadopoulos, V. Tangoulis, V. Psycharis, C. P. Raptopoulou, D. P. Kessissoglou, and G. Psomas, *J. Inorg. Biochem.*, 2012, **107**, 54-64.
- M. Ahmadi, T. Madrakian, A. Afkhami, *RSC Adv.*, 2015, **5**, 5450-5457.
- M. Ahmadi, T. Madrakian, A. Afkhami, *Sens. Actuators B: Chem.*, 2015, **210**, 439-445.
- L.J. Zhang, M.F. Song, Q. Tian, S.G. Min, *Sep. Purif. Technol.*, 2007, **55**, 388-391.
- Z.X. Zheng, J.M. Lin, F. Qu, *J. Chromatogr. A*, 2003, **1007**, 189-196.
- X.N. Lu, Y. Chen, L. Guo, Y.F. Yang, *J. Chromatogr. A*, 2002, **945**, 249-255.
- W. Liu and J. J. Gan, *J. Agric. Food. Chem.*, 2004, **52**, 755-761.
- J. Elek, D. Mangelings, T. Ivanyi, I. Lazar, Y.V. Heyden, *J. Pharm. Biomed.*, 2005, **38**, 601-608.
- L. Qi, G.I. Yang, H.Z. Zhang, J. Qiao, *Talanta*, 2010, **81**, 1554-1559.
- L. Chi, J.Z. Zhao, T.D. James, *J. Org. Chem.*, 2008, **73**, 4684-4687.
- Y.L. Wei, S.F. Wang, S.M. Shuang, C. Dong, *Talanta*, 2010, **81**, 1800-1810.
- W. A. Tao, F. C. Gozzo and R. G. Cooks, *Anal. Chem.*, 2001, **73**, 1692-1698.
- C. Roussel, M. Roman, F. Andreoli, A. Del Rio, R. Faure and N. Vanthuynne, *Chirality*, 2006, **18**, 762-771.
- C. D. Tran, D. Oliveira and S. Yu, *Anal. Chem.*, 2006, **78**, 1349-1356.
- Y. Wei, Y. Ren, J. Li, S. Shuang and C. Dong, *Analyst*, 2011, **136**, 299-303.
- Lei, J.-D.; Tan, T.-W. *Biochem. Eng. J.* 2002, **11**, 175-179
- H.S. Guo, J.M. Kim, S.M. Chang, W.S. Kim, *Biosens. Bioelectron.*, 2009, **24**, 2931-2934.
- Y. Huang, D. Guo, Q. Zhang, L. Guo, Y. Chen and Y. Fu, *RSC Adv.*, 2014, **4**, 33457-33461.
- Q. Chen, J. Zhou, Q. Han, Y. Wang, Y. Fu, *Colloids and Surfaces B: Biointerfaces*, 2012, **92**, 130-135.
- R. Nie, X. Bo, H. Wang, L. Zeng, L. Guo, *Electrochem Commun.*, 2013, **27**, 112-115
- L. Guo, Y. Huang, Q. Zhang, C. Chen, D. Guo, Ya Chen and Y. Fu *J. Electrochem. Soc.*, 2014, **161**, B70-B74.
- Q. Chen, J. Zhou, Q. Han, Y. Wang, Y. Fu, *J Solid State Electrochem.*, 2012, **16**, 2481-2485
- Q. Zhang, L. Guo, Y. Huang, Y. Wang, Q. Han and Y. Fu, *Anal. Methods*, 2013, **5**, 4397-4401
- N. F. Atta, A. Galal, F. M. Abu-Attia and S. M. Azab, *J. Electrochem. Soc.*, 2010, **157**, F116-F123.
- R. N. Goyal, V. K. Gupta, M. Oyama and N. Bachheti, *Talanta*, 2007, **72**, 976-983.
- T. quczak, *Electrochim. Acta*, 2009, **54**, 5863-5870.
- Y. Zhang, S. Asahina, S. Yoshihara and T. Shirakashi, *Electrochim. Acta*, 2003, **48**, 741-747.
- M. S. El-Deab, T. Sotomura and T. Ohsaka, *J. Electrochem. Soc.*, 2005, **152**, C730-C737.
- G. Hager and A. G. Brolo, *J. Electroanal. Chem.*, 2003, **550**, 291-301.
- N. F. Atta, A. Galal, E. H. El-Ads, *Analyst*, 2012, **137**, 2658-2668.